Geothermics 65 (2017) 255–268

Contents lists available at ScienceDirect

Geothermics

journal homepage: www.elsevier.com/locate/geothermics

Hydrothermal characterization of wells GRT-1 and GRT-2 in Rittershoffen, France: Implications on the understanding of natural flow systems in the rhine graben

C. Baujard [a,*], A. Genter [a], E. Dalmais [a], V. Maurer [a], R. Hehn [a], R. Rosillette [a], J. Vidal [b], J. Schmittbuhl [b]

[a] ES-Geothermie, 26 Boulevard du Président Wilson, F-67000 Strasbourg, France
[b] EOST, 5 rue René Descartes, F-67084 Strasbourg Cedex, France

ARTICLE INFO

Article history:
Received 18 July 2016
Received in revised form 17 October 2016
Accepted 1 November 2016
Available online 8 November 2016

Keywords:
EGS
ECOGI
Rittershoffen
Upper rhine graben
Stimulation
Hydro-thermal characterisation

ABSTRACT

An extended description of the implementation of the deep geothermal wells GRT-1 and GRT-2 respectively drilled in 2012 and 2014 in the framework of the ECOGI project is given. These wells located in Rittershoffen (France) offer a unique opportunity to gather high quality datasets on a deep geothermal system in the Upper Rhine Graben at the transition between the Buntsandstein sandstone and the Palaeozoic granite basement. We present the extensive logging and well testing program that was applied and focus on hydraulic and thermal characterization of the targeted deep reservoir. Well architectures of GRT-1 and GRT-2 are described. Temperature logs in both wells are discussed in details. In particular, temperature in the production well GRT-2 is shown to reach 177 °C at 3196 m MD at thermal equilibrium. Production tests of both wells, reservoir development strategy applied in well GRT-1 and circulation test realised between wells are analysed. Productivity and injectivity indexes of GRT-1 and GRT-2 are estimated: Post-stimulation injectivity of GRT-1 and productivity of GRT-2 are respectively estimated to 2.5 l/s/bar and 3.5 l/s/bar. Hydraulic properties of the reservoir are inferred from production tests. Implications for the characterization of the large scale natural hydro-thermal system are discussed.

1. Introduction

1.1. Project overview

ECOGI is the first industrial deep geothermal project in France aiming to produce overheated water from natural geothermal resource embedded at the interface between the Triassic sedimentary layers and the top crystalline fractured basement of the Upper Rhine Graben (Baujard et al., 2015) using an Enhanced Geothermal System (EGS).

In the framework of the ECOGI project, a geothermal doublet has been drilled, targeting a deep seated fault zone in the granitic basement. It is designed to produce hot water at 170 °C and to deliver a heat power of 24 MWth to the "Roquette Frères" bio-refinery located in Beinheim, in order to cover around 25% of the industrial heat needs. The heat is delivered using a 15 km transport loop.

The drilling site is located in Rittershoffen, a village located in the Upper Rhine Valley (Northern Alsace, France), 6 km east of Soultz-sous-Forêts, the well-known European EGS pilot site. The location of the project is shown in Fig. 1.

The project was initiated in 2004 thanks to the interest of Roquette Frères to supply its bio-refinery in Beinheim with renewable energy. A feasibility study concluded in 2011 that the geothermal potential of the area was significant. Furthermore, this study identified a potential geothermal target, constituted by a regional fault zone associated with high temperature gradients measured in pre-existing oil exploration wells. The first well GRT-1 was drilled as soon as the administrative authorizations could be gathered, from September 2012 to December 2012. Well testing and subsequent reservoir development operations were realised between January 2013 and June 2013. An additional seismic acquisition was achieved in August 2013, in order to secure the trajectory of second well GRT-2. This second well was drilled between May and July 2014. Well testing operations and a circulation test were carried out during August, September and October 2014. The construction of the 15 km long heat delivery loop and of the power

* Corresponding author.
E-mail address: clement.baujard@es.fr (C. Baujard).

http://dx.doi.org/10.1016/j.geothermics.2016.11.001

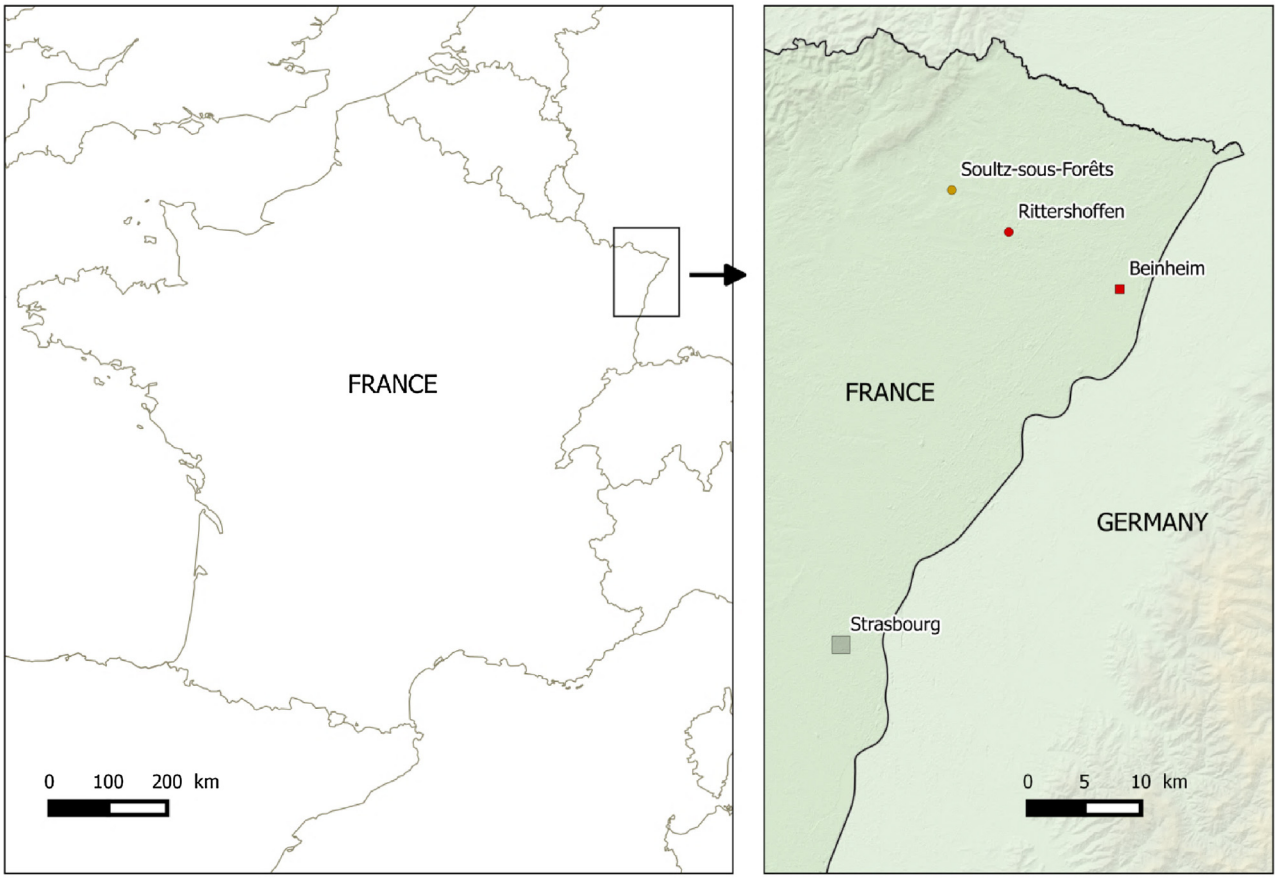

Fig. 1. Location of the ECOGI project: the deep geothermal reservoir for heat production is located in Rittershoffen (Northern Alsace, France), 6 km south-east of Soultz-sous-Forêts. The industrial site (Roquette Frères) where the heat will be used is in Benheim, 15 km. Heat will be transported between both site using a transport loop of overheated water.

plant started in February 2015. The geothermal plant went in operation by mid-2016.

1.2. Regional geological and geothermal settings

The Rittershoffen geothermal site is located 6 km south-east of the Soultz-sous-Forêts deep geothermal site where the overall geological, geophysical, geomechanical, geochemical features have been extensively studied (Kappelmeyer et al., 1992; Cornet et al., 2007; Dezayes et al., 2010; Genter et al., 2010; Bailleux et al., 2013, 2014). In summary, the site is within the Upper Rhine Graben (URG) which is part of the European Cenozoic rift system that extends from the Mediterranean to the North Sea coast. The site is located on the Western part of the URG at about 12 km form the major western Rhenane border fault. The URG's deep thermal structure, which is likely to be related to mantle uplift, shows an important rise up to 24 km depth in the southern URG (Edel et al., 2007). Extensive borehole data show that the temperature within the graben at depths of 1–2 km is highly variable, the thermal anomaly between Soultz and Rittershoffen being particularly high (Pribnow and Schellschmidt, 2000; Bailleux et al., 2013). Indeed, the shallow geothermal gradient in the graben ranges between 60 and 120 °C/km which corresponds to very high heat flow: up to 360 mW/m^2 assuming a typical thermal conductivity of 3 W/K/m and a purely conductive regime in the shallow crust (Pribnow and Schellschmidt, 2000).

The shallower geology of this area from 0 to 1500 m or 2200 m depth, respectively for Soultz and Rittershoffen (Georg Project Team, 2013), consists in Tertiary and Secondary sedimentary layers, overlaying a crystalline basement, constituted of altered and fractured granitic rocks from Carboniferous (Cocherie et al., 2004). Detailed geological analysis of the cuttings has shown that the top basement is located at about 2200 m MD (Measured Depth) in well GRT-1 (Aichholzer et al., 2015). The sedimentary layers are shifted by horst and graben structures with, in the vicinity of Rittershoffen, two horsts, Soultz in the west and Oberroedern in the East, enclosing a lower compartment in which the wells have been drilled (Georg Project Team, 2013).

Temperature, structural and stress conditions of the underground of the region are very well characterized thanks to numerous hydrocarbon exploration wells, to vintage seismic profiles and to extensive investigations that have been performed in the neighbouring geothermal site of Soultz-sous-Forêts (Genter et al., 2010; Dezayes et al., 2010; Place et al., 2010; Sausse et al., 2010; Valley, 2007).

During the 70′s and 80′s, several hydrocarbon exploration wells named R1–R4 and Oberroedern (OBR101) were drilled in this area (Fig. 3). They targeted deep-seated Triassic sedimentary layers, i.e. Muschelkalk limestone or Buntsandstein sandstone, or more shallowly tertiary layers, i.e. 'Couches de Pechelbronn' (Fig. 3). Most of these wells were unproductive for hydrocarbon but provided salty hot water (Munck et al., 1979). Temperatures derived mainly from drill stem tests show an overall geothermal linear gradient in the two first kilometers varying mainly between 7 and 9 °C/100 m (Fig. 4). Considering that these temperatures are often underestimated as they are acquired a few hours or days after drilling, the assumption of a gradient between 8.5 and 9 °C/100 m for Rittershoffen area was made before any geothermal drilling operations.

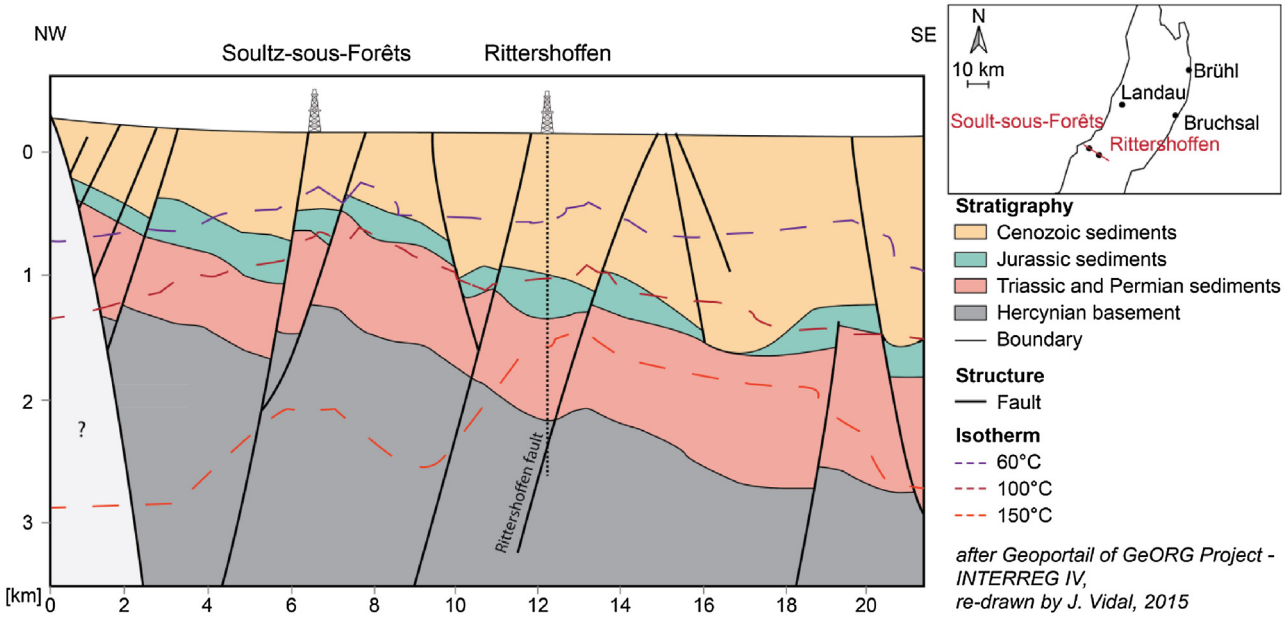

Fig. 2. NW-SE geological cross-section perpendicular to the graben axis between Soultz and Rittershoffen geothermal sites (Georg Project Team, 2013). The vertical dot line indicates an interpretative trajectory of GRT-1 that crosses the Rittershoffen fault.

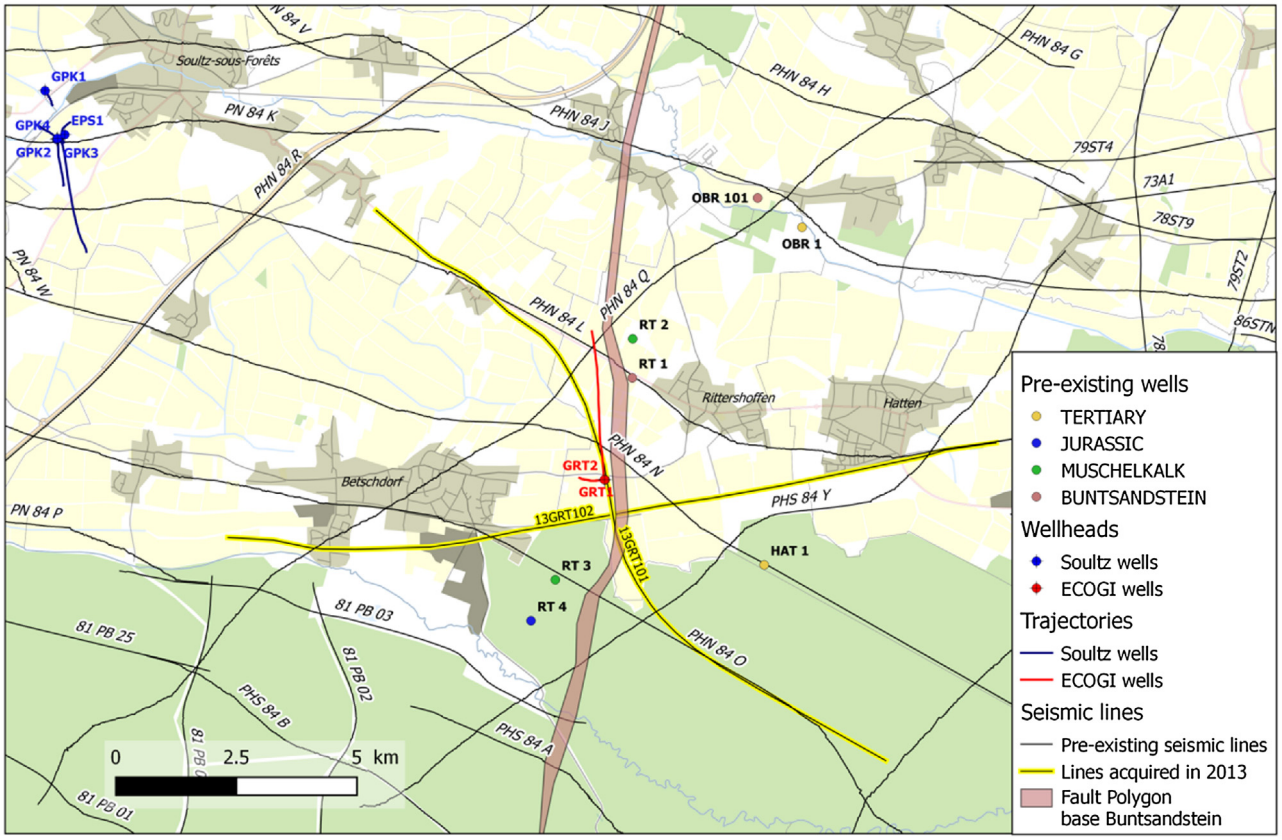

Fig. 3. Location and traces of pre-existing oil exploration wells, ECOGI and Soultz geothermal wells, pre-existing and recently acquired seismic data and target fault polygon at the base of the Buntsandstein (map background Open Street Maps).

Fig. 4 shows the measured temperatures of GRT1 and GRT2 at thermal equilibrium and confirms the relevance of the prediction (see Section 3 for an extended discussion).

The stress state to be found in the basement in this area is well known from various geophysical and mechanical measurements and interpretation derived from the area of Soultz (Valley, 2007; Cornet et al., 2007). Orientation of horizontal maximal stress S_H is approximately N169°E, whereas observations of focal mechanisms show a mix of normal and strike slip faulting suggesting that S_H is very closed to the vertical stress S_v (Dorbath, et al., 2010).

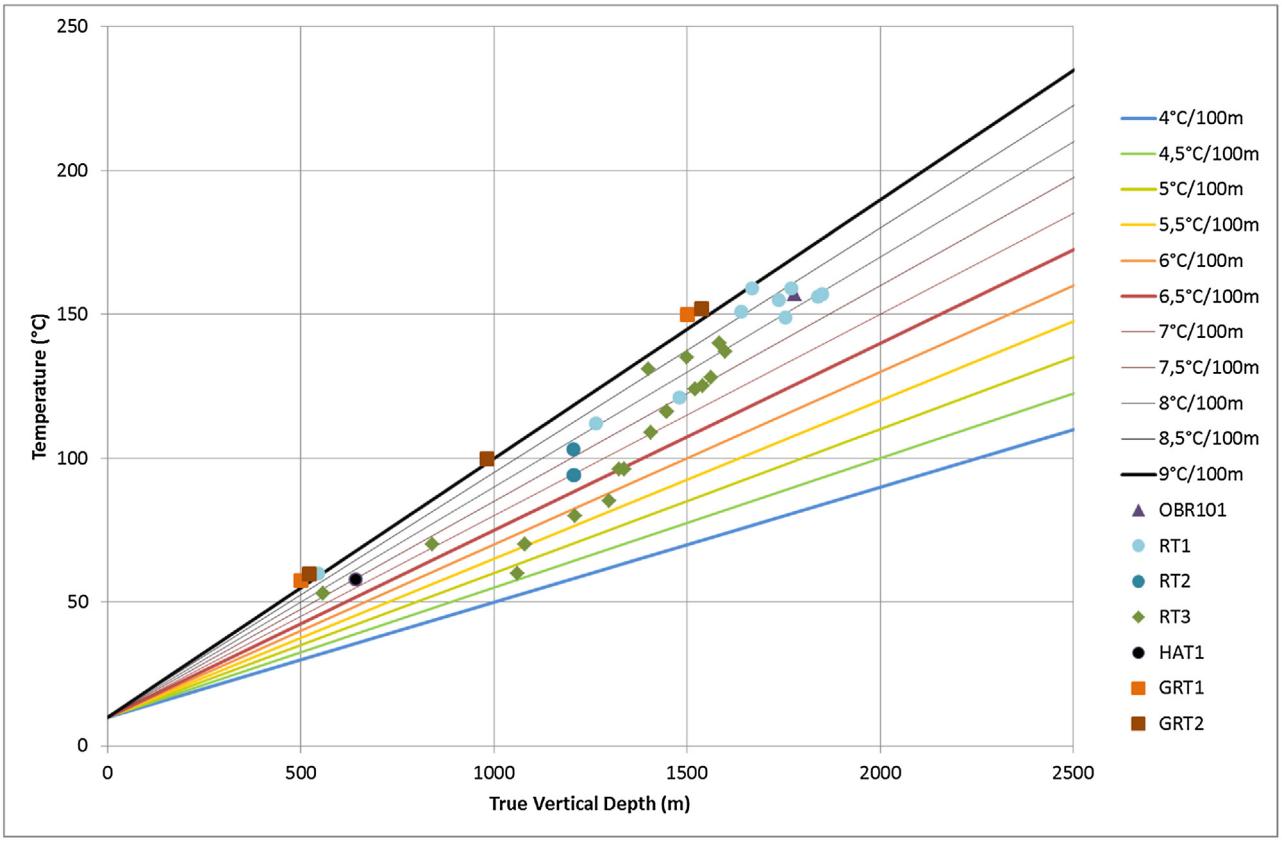

Fig. 4. Temperature versus depth from pre-existing oil wells drilled in Rittershoffen area (GRT-1 and GRT-2 temperatures are reported for comparison).

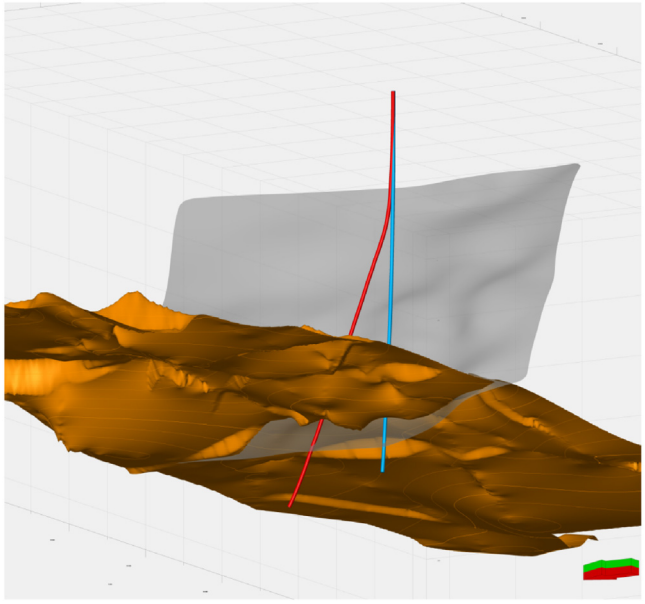

Fig. 5. 3D structural model based on seismic and well data showing GRT-1 (in blue – right side), GRT-2 (in red – left side), the Rittershoffen main fault structure (grey surface) and top granite basement (orange surface) at 2200 m TVD, viewed from below in the North/East direction. The red/green arrow indicates the north direction. (For interpretation of the references to colour in this figure legend, the reader is referred to the web version of this article.)

2. General description of wells GRT-1 and GRT-2

Both wells target the same fault zone, named Rittershoffen fault, in the crystalline basement (Fig. 2). This structure is relatively well known thanks to vintage seismic profiles from the 80's available in the vicinity of the project (see also Figs. 3 and 4) which were reprocessed in 2009, leading to an updated lithostructural and stratigraphic interpretation of the Rittershoffen region. It is a N355°E fault zone (becoming North-South at the well site), dipping 45° to the West, and showing an apparent vertical offset of more than 250 m (Fig. 5).

In both wells, the open-hole section crosses Buntsandstein and Permian clastic sandstones which covers a Paleozoic crystalline basement made of hydrothermally altered and fractured granite and intact granite.

The drilling of the first vertical well GRT-1 started in September 2012 and ended in December 2012 when the well reached a depth 2580 m MD within the fractured granite basement (see Fig. 6). The drilling rig was a MR8000 (hook load capacity 200To). No deviation tool was used. The maximum deviation is 8° to the West (see Fig. 5). Thus, GRT-1 intersects the Rittershoffen fault just below the top basement, roughly around 2400 m MD.

The drilling rig was demobilized after the first well in order to be able to perform a series of extended hydraulic tests and apply a coherent reservoir development strategy. Two new seismic profiles were acquired during summer 2013 in order to produce a better structural image of the reservoir for targeting the second well, GRT-2. Several post processing strategies were applied to this newly acquired seismic data which improved the geometrical understanding of the major local faults. Combined with the numerous logs and hydraulic tests performed in GRT-1 well, GRT-2 target has been identified and the trajectory designed.

The drilling of well GRT-2 started mid-March 2014. The drilling rig was a HH300 (280To). The final depth of 3196 m MD was reached end of July 2014. The well was slightly deviated using a downhole

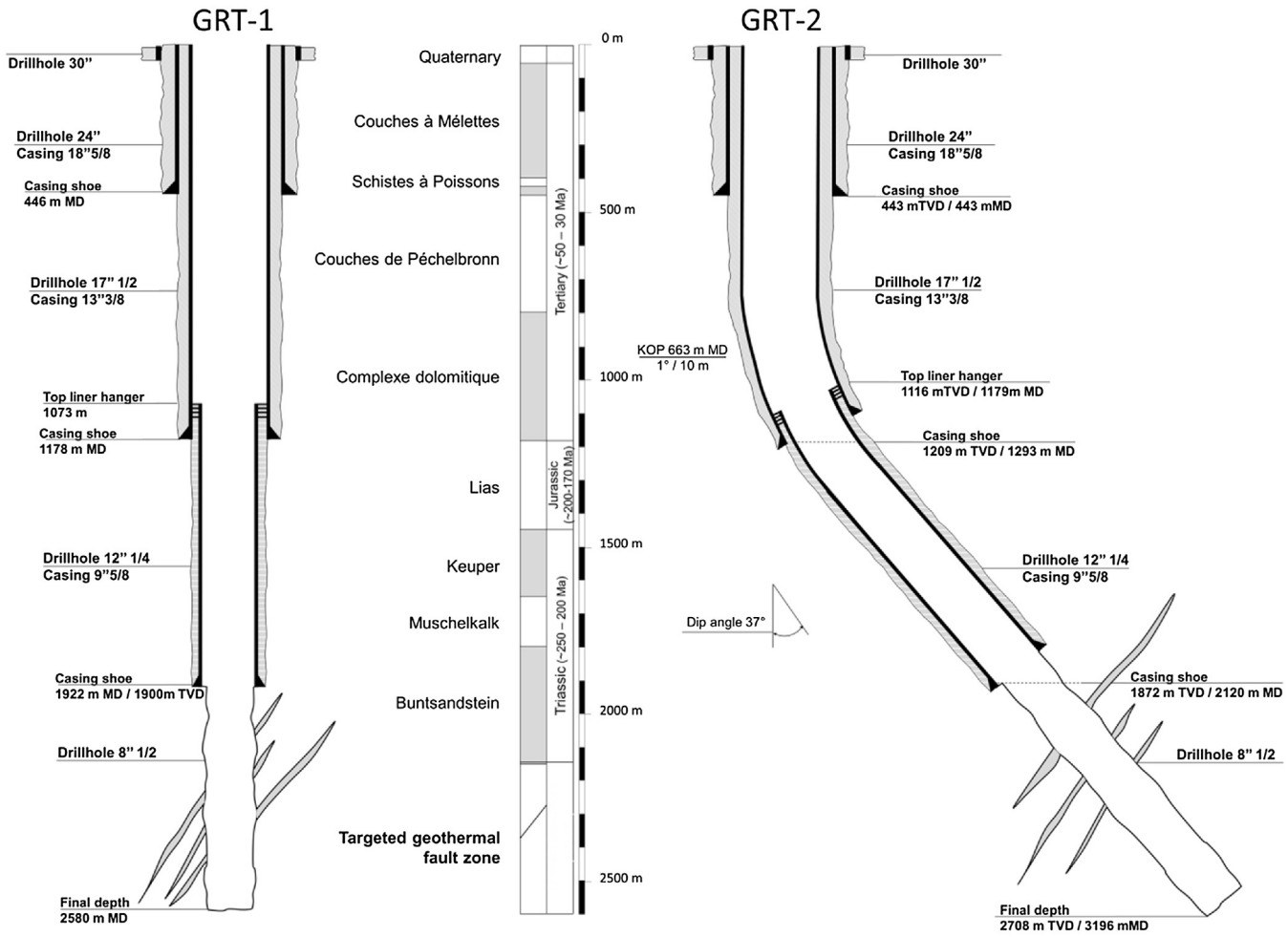

Fig. 6. GRT-1 and GRT-2 geothermal well completion and stratigraphic sequence. All depths are given from the surface.

mud motor. The inclination of the well reaches more than 37° and is directed to the north (Fig. 6).

The completion of both wells is very similar (Fig. 6). A conductor pipe was installed down to 40m depth prior to the drilling in order to avoid stability problems and protect groundwater from drilling mud losses. The first section (24″ hole diameter) was drilled in two stages (17″1/2 at first and the 24″ using a hole opener). The shoe of the 18″5/8 casing is set below the 'Schistes à Poisson' layer, known to be a regional aquifer. The 13″3/8 casing shoe is set at the base of the tertiary layers. The casing shoe of the 9/″58th liner is set at the base of the Muschelkalk. The hole diameter at target depth is 8″1/2; no perforated liner were used (the fully open section is in the Buntsandstein and granitic basement) in order to maximize well productivities.

3. Reservoir temperature

3.1. Measurement in well GRT-1

The most representative log of the thermal equilibrium profile was realised on April 22th 2013 (102 days after the well shut-in following the production tests in January 2013; the log was realised downwards). The maximum temperature at the bottom hole was measured at 163 °C at 2′526 m TVD (True Vertical Depth) (Fig. 7). From the surface approximately down to the top of the Muschelkalk, the temperature gradient is constant: 8.7 °C/100 m. It can be noted that this value is slightly lower than in Soultz-sous-Forêts where it reaches 11 °C/100 m (Genter et al., 2010; Vidal et al., 2015). At the top Muschelkalk, the temperature is about 160 °C (Fig. 7). Below the top Muschelkalk, the temperature profile changes very significantly despite a local small-scale positive anomaly. Indeed, the mean temperature gradient from the top Muschelkalk to the bottom of the well is very low: 0.3 °C/100 m which is about 30 times smaller than in the upper part of the well.

3.2. Measurement in well GRT-2

The most representative complete log of a thermal equilibrium profile in GRT-2 was measured in the cased well on September 08th 2014 (37 days after shut-in following the production sequence of the well; the log was performed downwards). The maximum temperature at the bottom hole in the granite section is 177.1 °C at 2′693 m TVD (Fig. 7). The thermal gradient shows very high values from the surface down to the top of the Muschelkalk with around 8.5 °C/100 m, very similarly to the temperature profile in GRT1, i.e. 8.7 °C/100 m. At the top of the Muschelkalk layers, the temperature reaches about 158 °C. Below the top Muschelkalk and down to the bottom hole, the thermal gradient is roughly constant despite several local perturbations and can be estimated to 1.8 °C/100 m. This value is significantly higher than for GRT-1, consistently with a higher bottom-hole temperature of the well. It must be emphasised that the well was probably not in a complete thermal steady-state when the temperature profile was acquired. Indeed, for GRT1, the waiting period before measuring the temperature log was

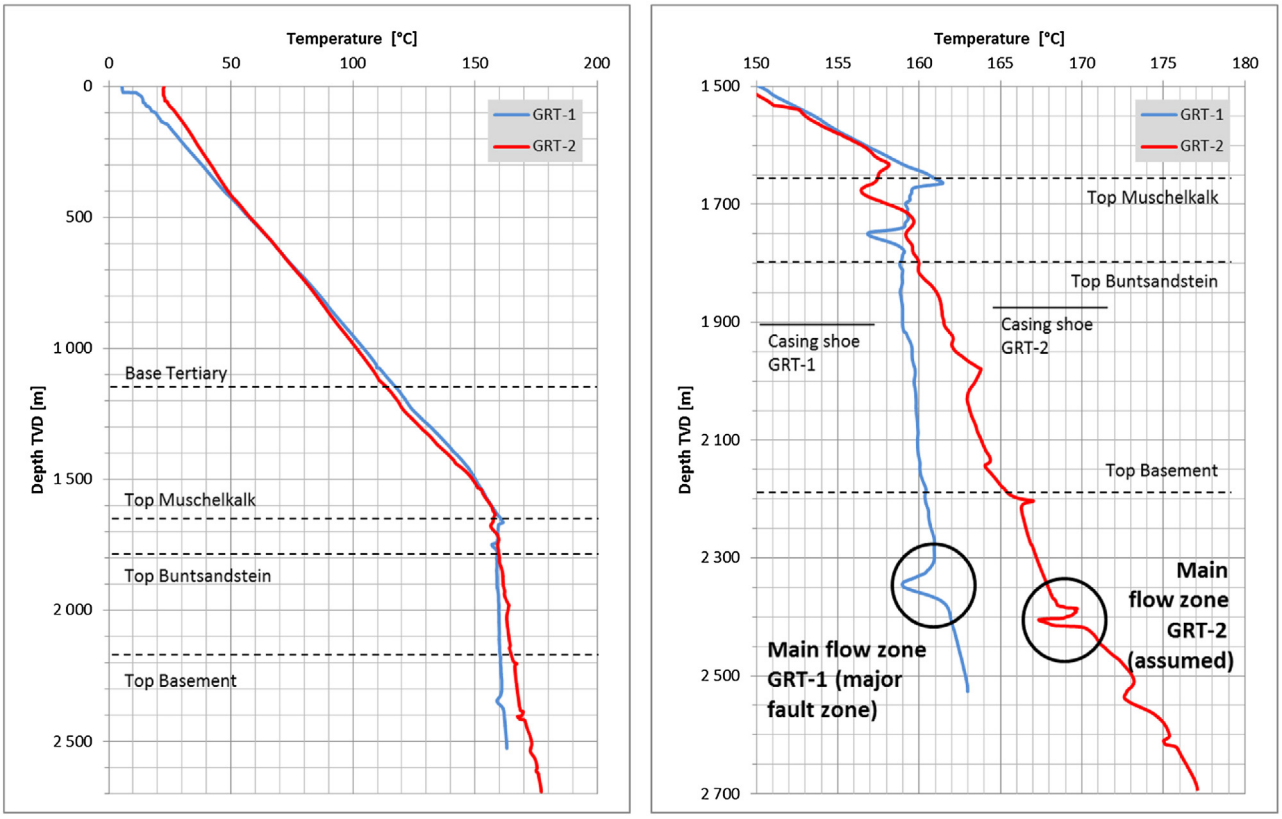

Fig. 7. Left: complete temperature profiles of GRT-1 and GRT-2; right: temperature profiles of GRT-1 and GRT-2 between the top Muschelkalk and the deep granite. Geological formation depths are indicative only as they may differ between the two geothermal wells (+/− 30 m).

comparable to the drilling period (about 3 months) which is typically a cooling period of the well owing to the drilling mud circulation. For GRT2, the waiting time is significantly shorter, only about 1/3 of the drilling period.

3.3. *Temperature logs comparison and implication on natural flows*

The general shape of both temperature profiles suggests a diffusive temperature regime from the ground surface to the top of the Muschelkalk formations and an advection-dominated temperature regime below the top Muschelkalk as proposed for the Soultz-sous-Forêts reservoir (Genter et al., 2010). This would suggest that the Keuper formations (mainly constituted of clays and dolomites), located directly above the Muschelkalk, act as a hydraulic barrier. The sharpness of the transition in the temperature profiles supports the existence of a barrier of caprock. The comparison between Soultz-sous-forêts and Rittershoffen where the Keuper formations are not at the same depth is of interest for addressing this question. At Soultz-sous-Forêts, the Keuper formations are at 860m and at 1650 m in GRT1. In both cases, it corresponds to the bottom end of the conductive regime. However, in Soultz-sous-Forêts, the transition to the convective regime is much smoother making it more difficult to associate specifically the correlation between the heat transport process change with the Keuper formations.

3.3.1. *Muschelkalk and Buntsandstein*

The temperature profile of GRT-1 shows two temperature anomalies in the Muschelkalk (a positive anomaly at the top of the formation, and a negative anomaly at the bottom). These anomalies could indicate that this formation host significant natural fluid circulations. This is supported by the fact that severe mud losses occurred in the Muschelkalk during drilling. This phenomenon is partly confirmed in GRT-2, where a negative temperature anomaly could be identified in the Muschelkalk. A high ROP (rate of penetration) was observed during the drilling operations of GRT-2 in the Muschelkalk, but no drilling mud losses were reported. This observation indicates that natural permeability in the Muschelkalk is very heterogeneous since wells are only separated in this formation by only a few hundred of meters.

In the Buntsandstein, a thermal positive anomaly can be identified in GRT-2 around 1980 m TVD, whereas no significant thermal anomaly could be seen in GRT-1.

3.3.2. *Granitic basement*

An important negative temperature anomaly is located in GRT-1 around 2350 m TVD in the granite section. The amplitude of the anomaly can be estimated to −2.5 °C (Fig. 7).

In GRT-2, five thermal anomalies with variable amplitudes were identified at 2200 m TVD, 2380 m TVD, 2400–2415 m TVD, 2530 m TVD and 2620 m TVD (Fig. 7). The most important temperature anomaly in the open-hole section of the well is observed in the granite section between 2′400 m TVD and 2′415 m TVD. The total amplitude of this negative anomaly is almost −3 °C. Interestingly, a positive anomaly is located directly above this negative anomaly, between 2′380 m TVD and 2′400 m TVD suggesting a strong lateral variability of the natural flows and subsequently significant channelling effects certainly related to large open fractures or faults.

The negative temperature anomaly located at 2′350 m TVD in the basement of GRT-1 is clearly correlated with a production zone according to spinner logs realised during a production test. Borehole image analysis also confirms the existence of a main fractured zone at that depth (Vidal et al., 2016). Unfortunately, no spinner log was performed in GRT-2, but the production temperature

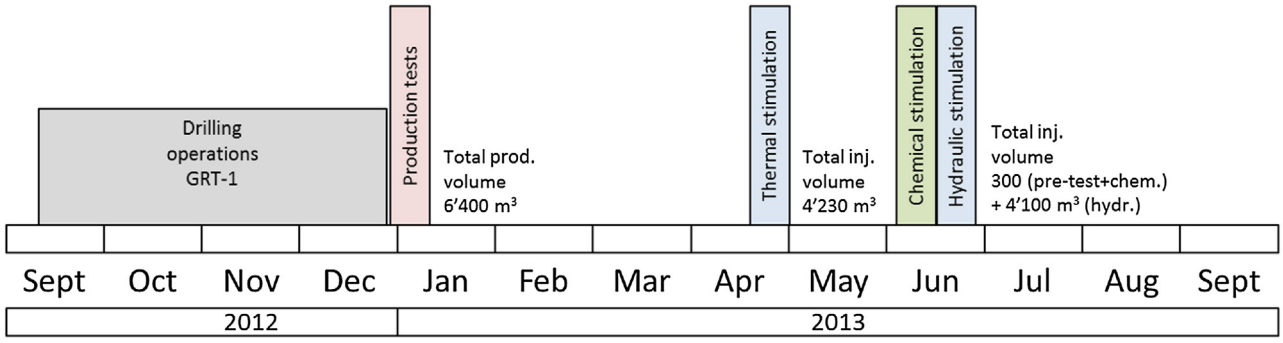

Fig. 8. GRT-1 well production tests and applied development strategy and total produced and injected volumes.

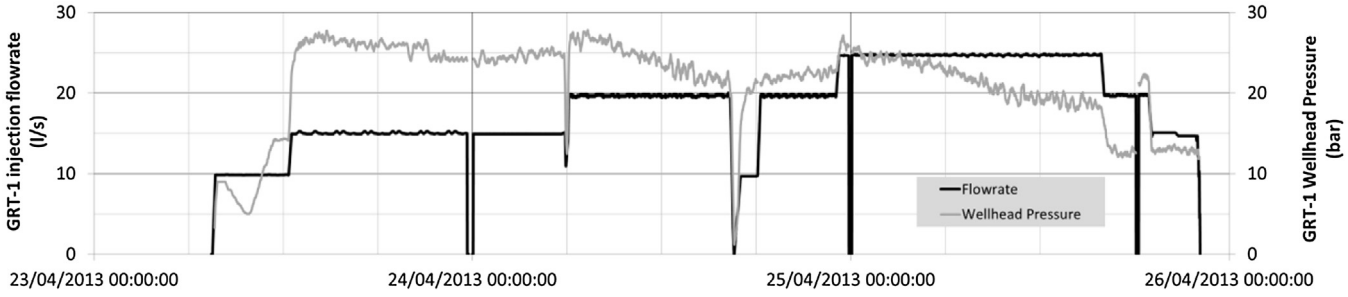

Fig. 9. Thermal stimulation of the geothermal well GRT-1 on April 2013.

during the circulation test (see below) reached 166 °C at the wellhead. This temperature value is compatible with a temperature of 168 °C at the production zone. Thus, it seems reasonable to assume that the temperature anomaly located around 2′400 m TVD in GRT-2 also corresponds to a main flow zone. These observations confirm that local fault zones of the Rhine Graben host natural fluid circulations.

The main difference between temperature profiles of both wells is the gradient value below the top Muschelkalk (see Fig. 7). The temperature gradient in GRT-1 is almost zero (0.3 °C/100 m) whereas it is significantly larger in GRT-2 (1.8 °C/100 m). This difference could be related to the difference in delay after the perturbations by the drilling fluid circulation, as the upper part of the 8′′1/2 section was cooled down longer than the deeper part (which might already have reached thermal equilibrium, contrarily to the upper part). The difference could also be related to the lateral variability of the temperature field in the reservoir. The comparison between both temperature profiles also shows that the temperature profile of GRT-2 is characterized by several positive thermal anomalies, for example at 2′200 m TVD and 2′380 m TVD (Fig. 7), that are not observed in GRT-1 where only negative anomalies are observed. These anomalies could be linked with the previous production test (see Section 4).

4. Hydraulic testing of the reservoir

4.1. Well GRT-1

4.1.1. Production tests

The well clean-up operations were realised between December 30th, 2012 and January 1st, 2013. 3′000 m³ were produced; the production started with an air-lift and continued with an artesian flow. No monitoring tool was installed in the well during this phase.

Following this well clean-up phase, a first air-lifted production test was performed between January 3rd and January 6th, 2013 (air injection at 300 m depth). A total of 3′000 m³ were produced. The PT (Pressure Temperature) probe had been placed close to the casing shoe at 1′910 m MD during production. The production flowrate was extremely erratic. In order to try to stabilize it, the test started with a 24 h production sequence at a maximal flowrate (14 l/s) to heat-up the well. Three descending short step-rates were then imposed (14 l/s, 11 l/s and 9,7 l/s, 3 h each). The maximum recorded downhole temperature was 157 °C. Unfortunately, the downhole measurements had to be interrupted before and during the build-up due to the necessity to cool-down the pressure probe at the surface. The PT logging tool was put in the well again during the build-up phase at 1′907.5 m MD. After a 12 h build-up, the test was continued with a sequence of 32 h of artesian production (average flowrate 10 l/s), but the downhole sensors failed and no downhole PT could be recorded during this production phase.

In order to get better data, a second production test was performed on January 9th and 10th. A total of 400 m³ were produced during this 12 h test. The production was air-lifted (air injection at 500 m depth, using a booster). Flowrate could be stabilised at 8 l/s and the downhole pressure during the build-up phase was fully recorded. The PT probe was positioned in the open-hole section at 2′298 m MD. The maximum recorded temperature at that depth was 158 °C.

Due to the erratic production flowrate and to a poor data quality, the interpretation of the pumping tests of GRT-1 is problematic. Nevertheless, the well productivity at this stage could be estimated to 0,45 l/s/bar.

4.1.2. GRT-1 well and reservoir development sequence

A reservoir development strategy was developed and applied. It consisted in three distinctive phases (Fig. 8). Firstly, a thermal stimulation (phase 1) of the well, with low-rate cold fluid injections was applied in April 2013. Then, a targeted chemical stimulation (phase 2) immediately followed by a hydraulic stimulation (phase 3) of the well were realised in June 2013.

The thermal stimulation (phase 1) of the well started on April 23rd 2013 at 07:40 and terminated on April 25th 2013 at 22:00 (Fig. 9). This stimulation consisted of a low-rate cold fluid injection into the well. A total fluid volume of 4′230 m³ was injected,

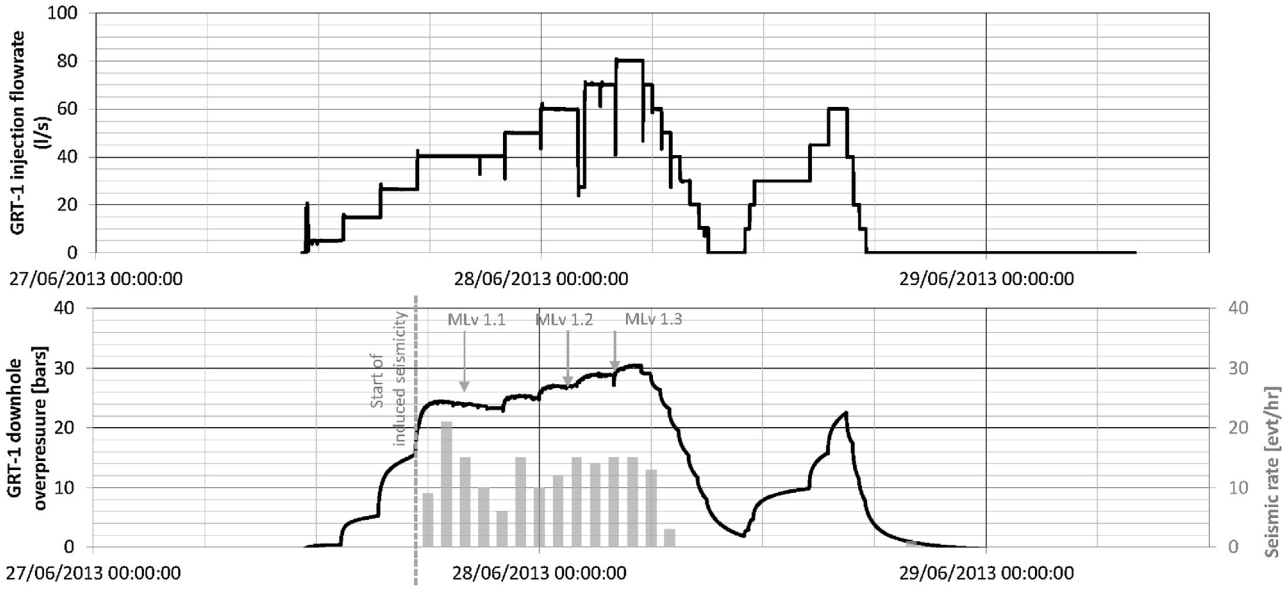

Fig. 10. Hydraulic stimulation sequence of GRT-1. The seismic rate is based on automatically detected events only. Main induced seismic events that occurred during injection are reported on the pressure curve (this figure does not show the post shut-in crisis).

at 6 different injection rates, ranging from 10 l/s to a maximum of 25 l/s. Injection temperature remained relatively constant to 12 °C. The maximum wellhead pressure recorded during this injection (no downhole tool was installed in the well) reached 28 bar. During this experiment, GRT-1 injectivity increased from an initial value of 0.6 l/s/bar to 1.3 l/s/bar at a flowrate of 20 l/s (see also Fig. 14). The injection generated 113 micro-earthquakes, with a maximum local magnitude (M_l) of 1.2 (Maurer, et al., 2015).

Phase 2 (chemical stimulation) and phase 3 (hydraulic stimulation) were realised consecutively. This stimulation experiment started on June 22nd 2013 and terminated on June 29th 2013. A total fluid volume of 4′400 m^3 was injected into the well. The sequence started with an injection test (3 constant flowrate steps of 5, 15 and 26.5 l/s) realised on June 22nd between 09:00 and 15:30. Downhole pressure was monitored using a logging tool at the casing shoe (1914 m MD).

Environmentally friendly acids were specifically designed for the chemical treatment of the well (phase 2), using drilling cuttings for laboratory testing (Recalde Lummer et al., 2014). The chemical stimulation was designed to dissolve the main hydrothermal minerals sealing the natural fractures. Clay minerals, secondary quartz, carbonates and sulphates were observed in the drilling cuttings from binocular observation, X-ray diffraction and thin sections. In order to avoid strong acids, it was decided to use glutamate-based chemicals able to dissolve calcite minerals (Recalde Lummer, et al., 2014). Mineralogical description and calcimetry based on cuttings were used for prioritizing the three main stimulated zones. The chemical injections were applied using open-hole packers at 5 l/s through 2“ coiled tubing, thus limiting the quantity of chemicals to be injected. No seismicity was detected during that sequence (Maurer, et al., 2015). Chemical injections were applied to three different depth intervals of the well, according to:

- From June 23rd – 16:00 to June 23rd – 23:00, 120 m^3 were injected to the first interval into the Basement (2′370–2′530 m MD).
- From June 24th 22:20 to June 24th 23:35, 42 m^3 were injected to the second interval into the Basement (2′300–2′335 m MD).
- From June 25th 14:00 to June 25th 19:00, 54 m^3 were injected to the third interval into the Buntsandstein (1′922–2′070 m MD).

The hydraulic stimulation (phase 3) was realised on June 27th and June 28th. In order to be able to quantify the effect of the chemical treatment, the three first injection steps were similar to the initial injection test realised on June 22nd. Maximum flowrates up to 80 l/s were applied during this stimulation sequence. The stepwise injection started on June 27th at 11:20 and terminated on June 28th at 09:00. It was consisted by 8 step rates injections, up to 80 l/s. The duration of the increasing steps was set up to a minimum of 2 h, and the decision to go to the next steps was based on the observed induced seismicity rate. The same injection steps were applied for the progressive shut-in, with a step length of one hour. On June 28th from 11:00 to 17:30, a short injection test was completed at the end of the stimulation to determine the final injectivity index (Fig. 10). The final injectivity index of the well could be estimated to 2,3–2,5 l/s/bar. An advanced seismological monitoring of the reservoir has been set up in collaboration with the University of Strasbourg (Maurer et al., 2015), allowing for real-time location of induced seismic events, thus offering the best support for decision makers during operation. In total, 212 induced events were automatically detected. The seismic activity started right after the flow rate exceeded 40 l/s meaning that the injection flow rate had to overtake the maximum injection flow rate of the thermal stimulation to generate a new micro-seismic activity. About 85 h after the last injection, while all activity was stopped on the platform, a sudden rise of seismic activity was observed during the shut-in period. A small crisis of 37 induced micro-seismic events was detected between the 2nd and the 4th of July. The largest micro-seismic event of the stimulation sequence occurred during this post-stimulation crisis and reached a magnitude M_l of 1.6 (Maurer, et al., 2015). The maximum magnitude threshold set (1.7 M_l) was never reached and no earthquake was felt by the local population.

The impacts of the thermal, chemical and hydraulic stimulations on the well are respectively estimated to factors 1.3, 2 and 1.5. The efficiency of the different stimulation sequences is discussed in Section 5.

4.2. Well GRT-2

The final depth of the well GRT-2 at 3196 m MD was reached on July 20th 2014. The first well cleaning operations were realised on July 25th and 26th using airlift (air injection at 300 m) and the total

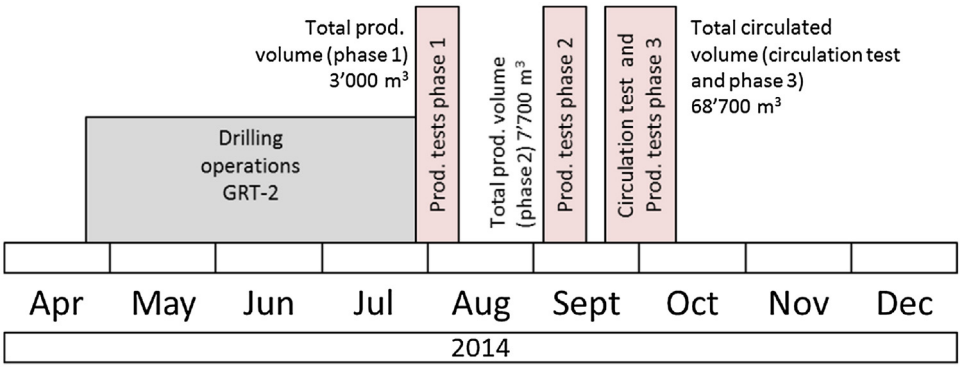

Fig. 11. GRT-2 well production tests and total produced and circulated volumes.

fluid volume produced reached 1′130 m^3, at a maximal flowrate of 54 l/s. During the logging operations, a well-logging tool could not reach the bottom of the well. Thus, it was decided to realise a well control by running a drill bit to the final depth in order to check the well integrity on July 27th and 28th. The operation run smoothly and final depth could be reached again. Then, standard acidizing (HCl) operations were realised on July 29th and July 30th. A total acid volume of 175 m^3 (KCl and HCl at 15% mixture) was injected and pushed in GRT-2 at 4 different depth intervals (Fig. 11).

4.2.1. Production test – phase 1

The first phase of production tests started on July 31st at 18:30. The well started to produce without any airlift. This testing phase was a step-rate test, aiming at reproducing the pumping test sequence applied for GRT-1. A total of 7 steps were performed at various flowrates. As for GRT-1, this sequence constitutes a stepwise procedure of decreasing flowrate. The objective was to characterize the near well reservoir and to derive a well productivity index. On the surface, the liquid flowrate was measured in a V-notch weir box, using an ultrasonic water level sensor. Pressure and temperature were measured at the wellhead, on the flow line and at the casing shoe (2110 m MD/1850 m TVD). The well was shut on August 1st 2014, at 17:00.

A total of 3′000 m^3 of geothermal fluid was produced during this test phase. Several problems were encountered during this production test:

- The downhole data are not consistent with the surface data (at least for pressure). The downhole pressure shows a constant decrease whereas the surface pressure and flowrate reach a steady state.
- The downhole pressure gauge stopped working after the step 7, implying that the build-up downhole data could not be recorded properly.

4.2.2. Production test – phase 2.1 (short production test)

New sensors were installed down to the casing shoe of GRT-2 (2′120 m MD), and a second step-rate test phase, denoted 2.1, was conducted. This time, it was decided to perform sequential steps of increasing flowrate (Fig. 12). The flow-line was modified in order to allow a better control of the flowrate and to eliminate vibrations. The downhole logging tool was located above the casing shoe (2091.3 m MD/1847.8 m TVD) and was equipped with two temperature and two pressure gauges in order to have a back-up in case of failure. Wellhead data are in agreement with downhole pressure data. A total of 1′670 m^3 of geothermal fluid (liquid phase only) was produced during this phase.

The initial downhole pressure value is 191.8 bar. After the test, the downhole pressure approximately stabilises at 190.1 bar. This difference can be explained by a change of density of the water column between reservoir depth and measurement depth. Indeed, the well is initially filled with a mix of geothermal brine and fresh water, as fresh water was injected into the well before the test in order to start production. The initial downhole temperature was 145 °C, whereas the wellwas filled with purely geothermal brine at the end of the test. Thus, assuming a 70% fresh water and 30% geothermal brine mixture at the beginning of the test (estimated resulting density at 145 °C: 942 kg/m^3 (Sharqawy et al., 2010) and a 100% geothermal brine at the end of the test (estimated density at 167 °C: 977 kg/m^3) leads to initial and final reservoir pressure estimations of respectively 242.8 bar and 243 bar at 2′400 m TVD.

4.3. Interference test – phase 2.2 (long production test)

This step-rate test was immediately followed by a 2.5 day production test, at approximately 28 l/s – liquid phase only (Fig. 12). The total liquid volume produced during this phase was 6′000 m^3. During this test, the downhole pressure/temperature was monitored in GRT-2 and in GRT-1. The well was very close to equilibrium as no production or injection had been realised in GRT-1 since the well was killed at the end of July 2014.

The downhole pressure in GRT-2 stabilises very quickly during production around 186.1 bar. At the end of the production, the pressure recovers to a level of 190 bar, very close to the initial pressure of 190.1 bar (still increasing when the logging tool was removed). The maximum recorded temperature during production is 169 °C at the casing shoe.

The downhole pressure recorded in GRT-1 shows a very clear tide signal. Thus, the signal was corrected using BETCO (Barometric Earth Tides Correction) software (Toll and Rasmussen, 2007). The input data were GRT-1 downhole pressure data, surface barometric pressure and earth tides values. The corrected pressure showed in Fig. 12 was obtained using a sampling interval of 15 mn and a maximum lag time of 8 h. After these corrections, it appears that recorded pressure in GRT-1 is clearly correlated with production in GRT-2 (see interpretation below).

4.4. Circulation test and production test – phase 3

Following phase 2, a three weeks circulation test has been conducted between wells GRT-1 and GRT-2. Injection in GRT-1 started on Sept. 16th at 8:35 and production from GRT-2 started on the same day at 10:00. Injection and production flowrates were kept relatively constant around 28 l/s until October 8th. Short breaks in production and injection for filter cleaning or production line cleaning occurred during this circulation test (Fig. 13).

Two different tracers were injected in GRT-1 on Sept. 18th: 200 kg of 2.7-naphthalene disulphonate (dissolved in 650 l of

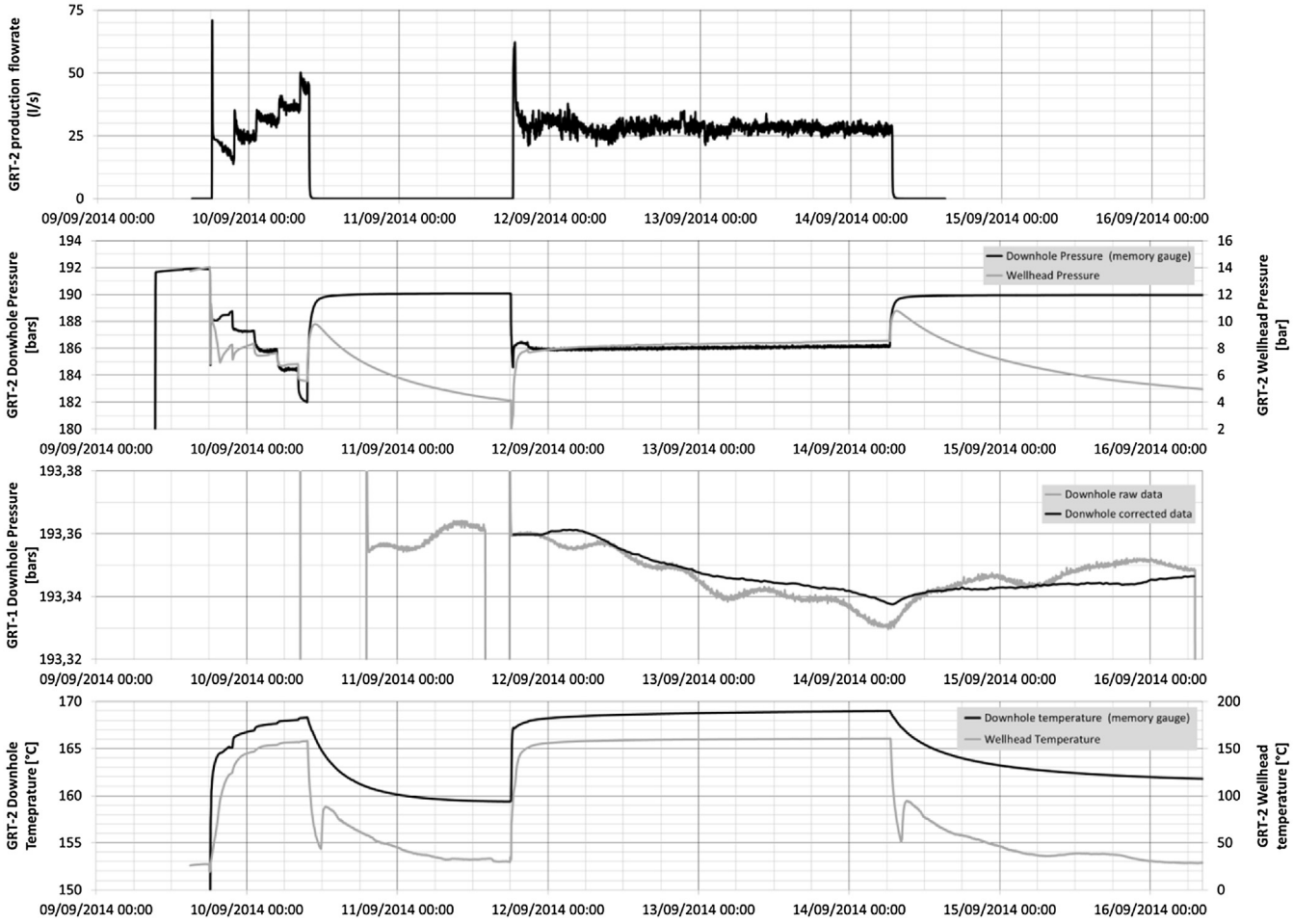

Fig. 12. GRT-2 production tests (phase 2.1 and phase 2.2).

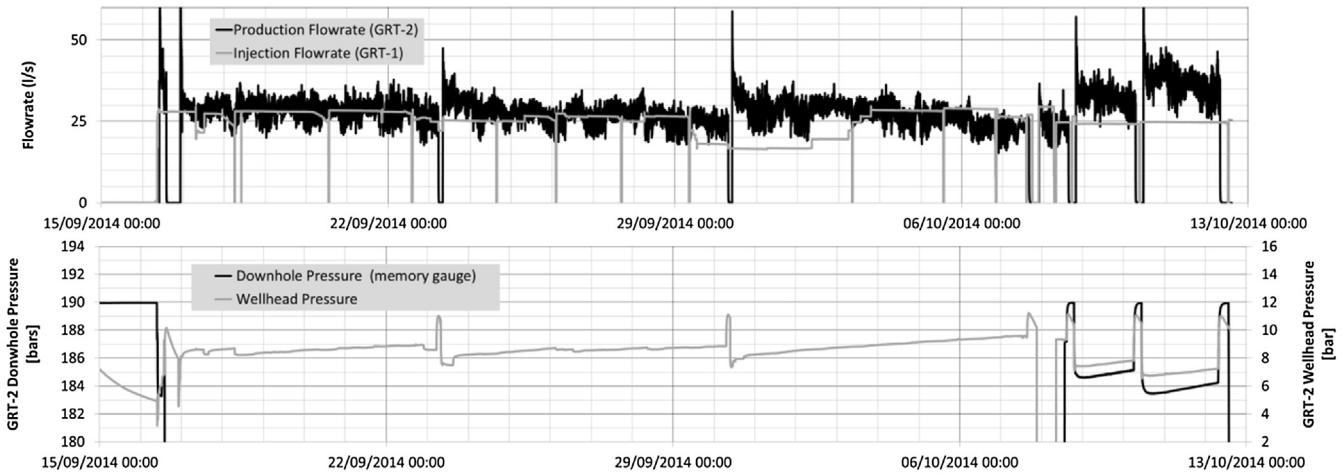

Fig. 13. Circulation test and production test – phase 3.

water) were injected at 9:00 am and 200 kg of fluorescein (dissolved in 700 l water) at 11:00 am The tracer breakthrough occurs on October 2nd, 14 days after injection, thus confirming the connection between GRT-1 and GRT-2 (Sanjuan, et al., 2016).

On October 8th, a downhole pressure gauge was set at the casing shoe GRT-2 at 2100 m MD, and a last GRT-2 production sequence (phase 3) was initiated. The purpose of this sequence was to confirm the well productivity after the three weeks circulation test. The initial pressure value measured is 189.96 bar (not stabilised). The injection in GRT-1 was continued at 25 l/s. A total of five production steps between 30 l/s and 42 l/s have been recorded during this phase. No induced seismicity was detected during this testing sequence (Maurer, et al., 2015)(Maurer, et al., 2015).

5. Inferred thermo-hydraulic properties and discussion

5.1. Injectivity and productivity indexes

The well development strategy applied on GRT-1 was successful. As a result, the injectivity of the well could be multiplied by a factor 5 to reach 2.5 l/s/bar at nominal flowrate of 70 l/s. The downhole overpressure versus the injection flowrate is showed in Fig. 14 for all injection phases. As no downhole pressure data were recorded during the thermal stimulation, a downhole pressure has been estimated using the fluid density measured at the surface (neglecting friction losses in the well as the flow-rate was quite low during this experiment). The final downhole differential pressure at nominal flowrate is estimated to 29 bar. The following observations can be made on this stimulation experiment:

- The thermal injection experiment clearly shows a well injectivity increase over time. The initial injectivity of the well using calculated downhole pressures is estimated to 0,6 l/s/bar, which is consistent with the measured initial productivity of the well (0,45 l/s/bar). The injectivity increase due to the thermal stimulation is almost permanent, as the pre-acidification step-rate test realised roughly 2 months later shows a similar injectivity.
- The chemical treatment had a clear impact on the well, as the low-rate steps realised at the beginning of the stimulation show lower injection pressure than the pre-acidification injections (see Fig. 14).
- Hydraulic stimulation had a big impact on the well, as the final injection tests show lower injection pressures than observed during the stimulation.

A clear change of the behaviour of the well can be observed during the hydraulic stimulation at flowrates above 40 l/s. Indeed, from that point, one can observe a linear increase of the downhole differential pressure with the flowrate. The question to know if this observation could be due to hydraulic fracturing processes in the reservoir has been investigated. It appears that this is not the case. Indeed, injection pressure at which this linear behaviour occurs is very low (between 23 bar and 31 bar overpressure during the stimulation and between 10 bar and 25 bar during the post stimulation injection test). The maximum absolute downhole pressure recorded during stimulation was 226.4 bar at 1′900 m TVD (corresponding to approximately 270 bar at 2′350 m TVD – assumed reservoir depth). In comparison, the minimal principal stress at that depth can be estimated to 316 bar, following the regional stress model based on experiments lead in Soultz-sous-Forêts (Cornet et al., 2007) or to 295 bar, considering only comparable depth values (Evans, 2005). Thus, the absolute reservoir pressure during injection remains below the minimal principal stress, confirming that hydraulic fracturing is not occurring during this stimulation phase. Moreover, the linear increase of pressure with injection flowrate could be reproduced during the final injection test and not only during stimulation. We would rather suggest that the stimulation sequence lead to the increase of near wellbore fracture aperture and permeability (in response to the reduced effective normal stress), resulting in connecting the well to a high-conductive feature (fractured reservoir).

Compared to the injectivity of GRT-1, the productivity of GRT-2 is very high. According to the different tests, the productivity index of GRT-2 is estimated to 2.8–3.5 l/s/bar at nominal flowrate. The downhole differential pressure at nominal flowrate (70 l/s) is estimated between 20 and 25 bar. Results obtained during all tests realised during the testing sequences 2.1, 2.2 and 3 are consistent with the fact that well GRT-2 is better connected to highly permeable features than GRT-1, through several drains (identified by the thermal anomalies in Fig. 4).

Table 1
Main hydraulic properties of the reservoir derived from pumping test interpretations based on Moench's model of double porosity with fracture skin effects (Moench, 1984). Fluid density is chosen as 970 kg/m^3 and reservoir thickness as 500 m (including a total fracture zone thickness of 40 m for GRT-2). Equivalent permeabilities are given in Table 2.

		GRT-1	GRT-2
Well	Dimensionless skin factor [–]	21.3	1.8
Fault	Hydraulic cond. [m s^{-1}]	–	$2.9{\cdot}10^{-06}$
	Specific storage [m^{-1}]	–	$7.2{\cdot}10^{-07}$
Matrix	Hydraulic cond. [m s^{-1}]	$6.1{\cdot}10^{-08}$	$5.3{\cdot}10^{-07}$
	Specific storage [m^{-1}]	$7.2{\cdot}10^{-07}$	$5.2{\cdot}10^{-07}$

5.2. Reservoir properties

In order to characterize hydraulic properties of the reservoir, classical pressure transient analysis interpretations have been carried out with pumping test data from each well using AQTESOLV software based on the direct use of analytical solutions (Baujard et al., 2016). For GRT-1, only downhole drawdown data of the 9/01/2013 and both recovery data of the 5/01/2013 (unfortunately incomplete) and of the 9/01/2013 have been interpreted. As the data quality is quite poor, the interpretation of GRT-1 production tests was realised using a single permeability confined aquifer model (Dougherty and Babu, 1984). For GRT-2, the step-drawdown test (phase 2.1) as well as drawdown and recovery data (phase 2.2) have been used for the interpretation. This time, the best results are obtained using a fractured confined aquifer model based on a double porosity approximation including a fracture skin effect (Moench, 1984). Observations realised in GRT-1 during GRT-2 test phase 2.2 have been taken into account (GRT-1 acting as an observation well) and measurements could be reproduced by the model. Main interpretation results are summarized in Table 1. Even though different models were applied to interpret these pumping tests, the following conclusions could be drawn from these works:

- GRT-1 is characterized by a high fracture skin coefficient (Horne, 1995) in comparison with GRT-2, meaning a low permeability in the near-well domain and a bad connection with the reservoir. These observations realised prior to the hydraulic stimulation of GRT-1, were largely confirmed by the stimulation results, leading to a drastic enhancement of near-well hydraulic properties and the development of a good connection with the reservoir.
- Reservoir properties derived from GRT-1 production tests are very different from values derived from GRT-2; GRT-1 seems so be badly connected to a medium permeability reservoir, whereas GRT-2 is connected to a highly permeable reservoir.
- No limit (no-flow or constant head boundary) could be identified in the data with the interpretations realised so far on GRT-1 or on GRT-2.

It must be underlined that GRT-1 production tests were quite short, and the production flowrates relatively low. Thus, the production tests are strongly influenced by near-well processes and head losses.

These tests also clearly demonstrate the existence of a hydraulic and of a mass (i.e. tracer) connection between GRT-1 and GRT-2 (see Fig. 12 and Section 4.d). On one hand, the hydraulic connection is quite fast, as, according to the pressure response recorded in GRT-1 during test phase 2.2, it seems that the pressure in GRT-1 starts to stop decreasing around 30 min after shut-in of GRT-2. On the other hand, the tracer breakthrough occurred 14 days after injection of the tracer. This period is very long in comparison with what has

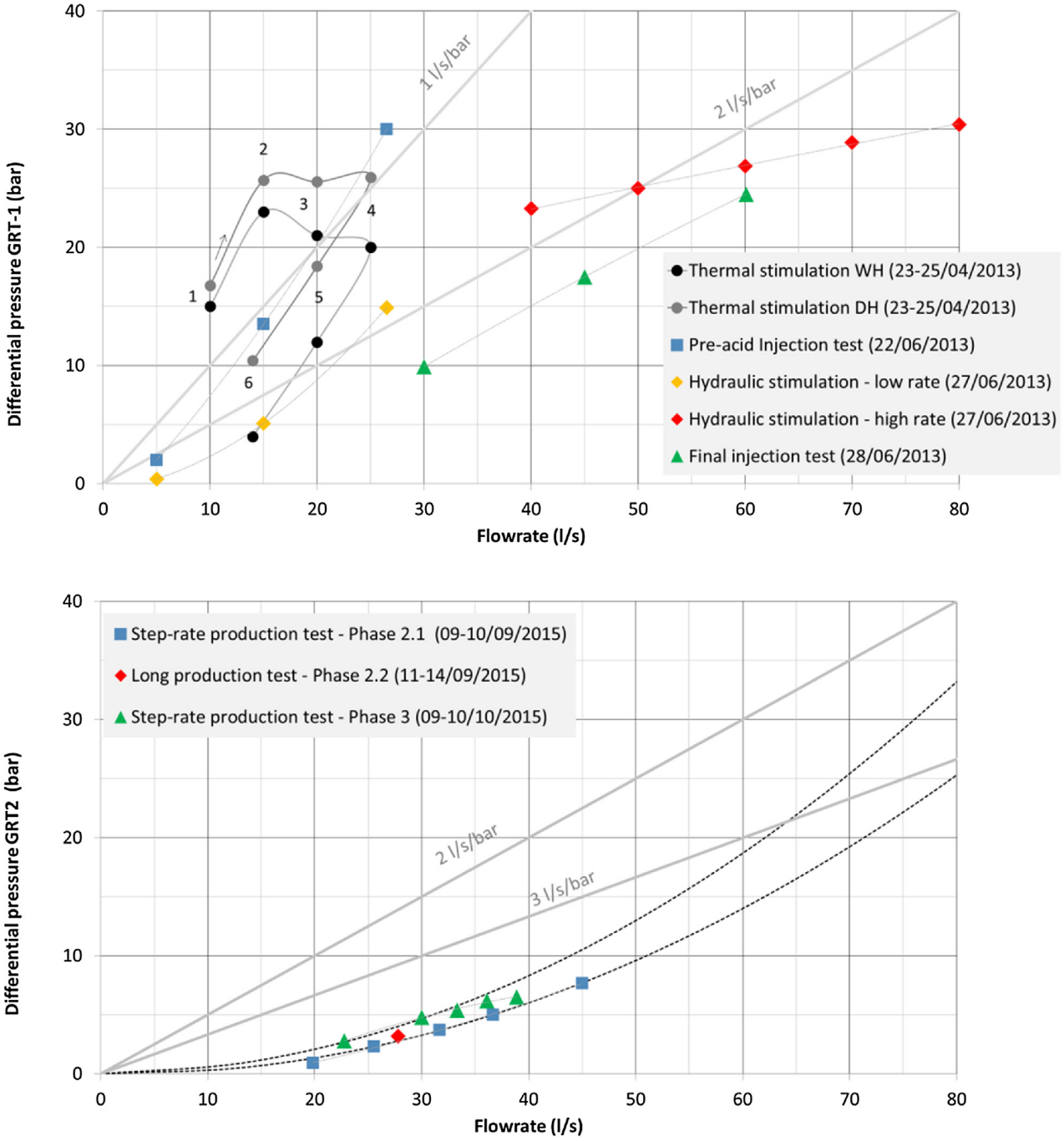

Fig. 14. GRT-1 injectivity index (top) and GRT-2 productivity index (bottom). Only liquid phase is considered in productivity index computation. All pressures are downhole differential pressures, except for the thermal stimulation experiment, for which a downhole overpressure is estimated ("Thermal stimulation DH") from the surface absolute pressure ("thermal stimulation WH"), using an estimation of the water column density.

been observed in Soultz-sous-Forêts between the best connected wells GPK-2 and GPK-3 (Sanjuan, et al., 2006).

5.3. Natural hydro-thermal convection

In order to investigate the possibility of occurrence of convection cells within the reservoir, the Rayleigh number has been calculated in the matrix and in the fault zone using the following formulation of the Rayleigh-Benard instability in a porous medium (Turcotte and Schubert, 2014):

$$Ra = \frac{\alpha_f g \rho_f^2 C_{pf} k b (T_1 - T_0)}{\mu \lambda_m}$$

With α_f [K^{-1}] the fluid thermal expansion coefficient, g [$m\,s^{-2}$] the gravity acceleration, ρ_f[$kg\,m^{-3}$] the fluid density, C_{pf} [$J\,kg^{-1}\,K^{-1}$] the fluid heat capacity, k [m^2] the reservoir permeability, b [m] the depth interval in which convection occurs, T_1 [K] the lower boundary initial temperature, T_0 [K] the upper boundary initial temperature, μ [Pa s] the fluid dynamic viscosity and λ_m [W/m/K] the reservoir thermal conductivity.

The values of the parameters used for the calculation and the resulting Rayleigh number are showed in Table 2. A lower boundary depth at 3000 m and a lower boundary temperature of 177 °C are assumed in the calculations. The upper boundary depth is set to

Table 2
Parameters used and resulting Rayleigh Number value. Hydraulic conductivity values are derived from pumping test interpretations of GRT-1 and GRT-2 (see Table 1).

			GRT1 Matrix	GRT2 Matrix	GRT2 Fracture
α	Fluid thermal expansion coefficient	$[K^{-1}]$	$1.50{\cdot}10^{-03}$		
g	Gravity acceleration	$[m\,s^{-2}]$	9,8		
ρ	Fluid Density	$[kg\,m^{-3}]$	970		
cp	Fluid heat capacity	$[J\,kg^{-1}\,K^{-1}]$	3800		
μ	Fluid dynamic viscosity	[Pa·s]	$1.75{\cdot}10^{-04}$		
λ	Matrix thermal conductivity	$[W{\cdot}m^{-1}\,K^{-1}]$	3		
K	Hydraulic conductivity	m/s	$6.00{\cdot}10^{-08}$	$5.00{\cdot}10^{-07}$	$2.90{\cdot}10^{-06}$
k	Permeability	$[m^2]$	$1.10{\cdot}10^{-15}$	$9.20{\cdot}10^{-15}$	$5.34{\cdot}10^{-14}$
Z0	Upper boundary depth of convection zone	[m]	1650		
Z1	Lower boundary depth of convection zone	[m]	3000		
b	Depth interval of convection zone	[m]	1350		
T1	Lower boundary initial temperature	[°C]	177		
T surf	Mean surface temperature	[°C]	12		
∇T	Initial temperature gradient	[K/m]	0.055		
T0	Upper boundary initial temperature	[°C]	102.8		
DT	Delta temperature	[K]	74.25		
Ra	**Rayleigh number**	**[–]**	**11.1**	**92.4**	**535.7**

1650 m (top of the Muschelkalk formation) and the upper boundary temperature is calculated assuming a 12 °C mean surface temperature and a constant temperature gradient (calculated from the lower boundary depth and temperature). Three different cases have been calculated based on the hydraulic conductivity derived from the production tests of GRT-1 (matrix only) and GRT-2 (matrix and fracture zone).

According to (Turcotte and Schubert, 2014), the critical Rayleigh number value at which convection could occur is 39.5. Thus, the results show that convection is very likely to occur with a permeability value of the fault zone derived from GRT-2 production tests. Rayleigh number values calculated using permeability values of the matrix derived from GRT-1 and GRT-2 production test do not allow to draw clear conclusions as they are quite close to the critical value and because of the oversimplified model that is considered. A more precise estimate taking into account the fault geometry i.e. a porous medium between two narrow facing walls should be considered.

6. Conclusions and discussion

Several important conclusions can be drawn after the results observed in this EGS project in Rittershoffen:

- First of all, the two wells GRT-1 and GRT-2 show respectively high injectivity and productivity indexes, reaching the economic threshold for exploitation. The geothermal target identified (regional fault zone in the basement associated with high temperature gradients) could be confirmed.
- Furthermore, the well development strategy applied to GRT-1 was very successful, as the injectivity index was increased by a factor 5, and the induced seismicity was limited, as no event could be felt by inhabitants.
- The correlation between different observations (mostly UBI acoustic imaging logs, temperature logs, flow-logs) confirms that regional fault zones in the Rhine Graben are permeable structures and host natural fluid circulations.
- Temperature logs in both wells show a clear contrast between the upper part and the lower part of the reservoir. The transition at Rittershoffen corresponds to the Keuper formations. The upper part hosts a conductive regime with a very constant high gradient (85 °C/km). Below the top of the Muschelkalk formation, heat transport is dominated by advective and/or convective processes, in particular in the vicinity of the regional fault structure.
- This conclusion is confirmed by the Rayleigh Number calculated in the fracture zone using estimated hydraulic properties from hydraulic tests. It is higher than the critical Rayleigh Number, thus showing that convection is likely to occur in these fault zones.
- On a purely mechanical point of view, it is also clear that the successful stimulation of GRT-1 is only due to hydroshearing mechanisms and that no hydraulic fracturing was observed during the stimulation.
- A mass and hydraulic connection between wells GRT-1 and GRT-2 could be highlighted by the interference and circulation/tracer tests performed

The following observations would need further investigations:

- Even if no production test was carried out on well GRT-1 after the stimulation and no injection test was realised in GRT-2, the wells show quite different productivity/injectivity indexes. This difference tends to demonstrate that GRT-2 is better connected to highly permeable features. The pressure evolution in GRT-1 during stimulation raises the question to know if this well really hits the regional fault zone or only a secondary feature. In this case, the hydraulic stimulation would have developed the connection with the main feature.
- An interesting observation has been done on the temperature logs. Indeed, it appears that several thermal anomalies are constituted by a positive anomaly at the top and a negative anomaly at the bottom. For example, the most important thermal anomaly in GRT-2 at 2′400 m TVD shows a 1 °C temperature increase between 2′380 m and 2′400 m and a 2–3 °C temperature decrease between 2′400 and 2′420 m TVD. This would suggest the existence of convection cells within a 40 m wide fault zone with ascending hot fluids on the top of the fault zone and descending 'cold' fluids on the bottom of the zone. A possible small scale convection within the fault zone has not been investigated in this paper.
- It is interesting to observe that the temperature profile of GRT-1 is nearly vertical below the top of the Muschelkalk (the temperature gradient value is 0,3 °C/km). On the contrary, the temperature gradient in the same horizons in GRT-2 is significantly larger (1.8 °C/100 m). The implication of this observation (if not only due to non-equilibrium conditions) has not be investigated.
- The question to know if the fault zone could have been targeted at shallower depth of 1600m (in the Muschelkalk) is open. The temperature profile strongly suggests that the Muschelkalk formation host natural fluid flow and that it could show high permeabilities, as suggested by the mud losses met during GRT-1. That being said, one must keep in mind that the Muschelkalk is likely to show strong lateral heterogeneities, and that the layer

is quite thin in comparison with the Bundsandstein; thus constituting a challenging target.

Acknowledgements

The authors would like to thank ECOGI, which is a joint venture between “Electricité de Strasbourg”, “Roquette Frères”, and “Caisse des Dépôts et Consignation”. The authors also warmly acknowledge researchers of the EOST team in Strasbourg (“Ecole et Observatoire des Sciences de la Terre”), which is a main actor of the Labex (“Laboratoire d’Excellence”) G-Eau-Thermie Profonde for fruitful discussions and scientific support. The works described in this paper are supported by “ADEME” with the “Fonds Chaleur” as well as the “EGS Alsace” research program. A part of this work was done in the framework of the DESTRESS Eu project which has received funding from the European Union’s Horizon 2020 research and innovation program under grant agreement No 691728.

References

Aichholzer, C., Duringer, P., Orciani, S., Genter, A., 2015. New stratigraphic interpretation of the twenty-eight-year old GPK-1 geothermal well of Soultz-sous-Forêts (Upper Rhine Graben, France). 4th European Geothermal Workshop EGW. Strasbourg.

Bailleux, P., Schill, E., Edel, J., Mauri, G., 2013. Localization of temperature anomalies in the Upper Rhine Graben: insights from geophysics and neotectonic activity. Int. Geol. Rev. 55 (14), 1744–1762.

Bailleux, P., Schill, E., Abdelfettah, Y., Dezayes, C., 2014. Possible natural fluid pathways from gravity pseudo-tomography in the geothermal fields in Northern Alsace (Upper Rhine Graben). Geotherm. Energy 2 (1), 1–14.

Baujard, C., Genter, A., Maurer, V., Dalmais, E., Graff, J.-J., 2015. ECOGI a new deep EGS project in Alsace, Rhine graben, France. In: World Geothermal Congress, Melbourne, Australia, 19–25 April 2015.

Baujard, C., Genter, A., Dalmais, E., Maurer, V., Hehn, R., Rosillette, R., 2016. Temperature and hydraulic properties of the Rittershoffen EGS Reservoir. In: France European Geothermal Conference, 19–24 Sept. 2016 Strasbourg, France.

Cocherie, A., Guerrot, C., Fanning, M., Genter, A., 2004. Datation U-Pb des deux faciès du granite de soultz (Fossé Rhénan, France). C.R. Geosci. 336, 775–787.

Cornet, F., Bérard, T., Bourouis, S., 2007. How close to failure is a granite rock mass at a 5 km depth? Int. J. Rock Mech. Min. Sci. 44, 47–66.

Dezayes, C., Genter, A., Valley, B., 2010. Structure of the low permeable naturally fractured geothermal reservoir at Soultz. C.R. Geosci. 342, 517–530.

Dorbath, L., Evans, K., Cuenot, N., Valley, B., Charléty, J., Frogneux, M., 2010. The stress field at Soultz-sous-Forêts from focal mechanisms of induced seismic events: cases of the wells GPK2 and GPK3. C.R. Geosci. 342 (7), 600–606.

Dougherty, D., Babu, D., 1984. Flow to a partially penetrating well in a double-porosity reservoir. Water Resour. Res. 20 (8), 1116–1122.

Edel, J.-B., Schulmann, K., Rotstein, Y., 2007. The Variscan tectonic inheritance of the Upper Rhine Graben: evidence of reactivations in the Lias, Late Eocene-Oligocene up to the Recent. Int. J. Earth Sci. 96, 305–325.

Evans, K., 2005. Permeability creation and damage due to massive fluid injections into granite at 3.5 km at Soultz: 2. Critical stress and fracture strength. J. Geophys. Res. 110, 14, http://dx.doi.org/10.1029/2004JB003169.

Genter, A., Evans, K., Cuenot, N., Fritsch, D., Sanjuan, B., 2010. Contribution of the exploration of deep crystalline fractured reservoir of Soultz to the knowledge of Enhanced Geothermal Systems (EGS). C.R. Geosci. 342, 502–516.

Georg Project Team, 2013. Potentiel géologique profond du Fossé rhénan supérieur. In: Open File Report BRGM/RP-61945-FR. Georg Project Team http://www.geopotenziale.eu.

Horne, R., 1995. Modern Well Test Analysis: A Computer-Aided Approach, 2nd edition. Petroway.

Kappelmeyer, O., Gérard, A., Schloemer, R., Ferrandes, F., Rummel, F., Benderitter, Y., 1992. Geothermal Energy in Europe – The Soultz Hot Dry Rock Project. Grodon and Breach Science Pu.

Maurer, V., Cuenot, N., Gaucher, E., Grunberg, M., Vergne, J., Wodling, H., et al., 2015. Seismic Monitoring of the Rittershoffen EGS Project (Alsace, France). World Geothermal Congress, Melbourne, Australia.

Moench, A., 1984. Double-porosity models for a fissured groundwater reservoir with fracture skin. Water Resour. Res. 20 (7), 831–846.

Munck, F., Walgenwitz, F., Maget, P., Sauer, K., Tietze, R., 1979. Synthèse géothermique Du Fossé Rhénan Supérieur. BRGM Service Géologique Régional d’Alsace -Geologisches Landesamt Baden-Württemberg. Commission of the European Communities.

Place, J., Diraison, M., Naville, C., Géraud, Y., Schaming, M., Dezayes, C., 2010. Decoupling of deformation in the upper rhine graben sediments. seismic reflection and diffraction on 3-component vertical seismic profiling (Soultz-sous-Forêts area). C.R. Geosci., 575–586.

Pribnow, D., Schellschmidt, R., 2000. Thermal tracking of Upper crustal fluid flow in the Rhine Graben. Geophys. Res. Lett. 27, 1957–1960.

Recalde Lummer, N., Rauf, O., Gerdes, S., Genter, A., Scheiber, J., Villadangos, G., 2014. New biodegradable stimulation system – First field trial in granite/Bunter sandstone formation for a geothermal application in the Upper Rhine Valley. In: Deep Geothermal Days., Paris, France.

Sanjuan, B., Pinault, J., Rose, P., Gerard, A., Brach, M., Braibant, G., et al., 2006. Tracer testing of the geothermal heat exchanger at Soultz-sous-Forêts (France) between 2000 and 2005. Geothermics 35 (5–6), 622–653.

Sanjuan, B., Scheiber, J., Gal, F., Touzelet, S., Genter, A., Villadangos, G., 2016. Interwell chemical tracer testing at the Rittershoffen site (Alsace, France). In: European Geothermal Conference EGC, Strasbourg, France.

Sausse, J., Dezayes, C., Dorbath, L., Genter, A., Place, J., 2010. 3D fracture zone network at Soultz based on geological data, image logs: microseismic events and VSP results. C.R. Geoscience 342, 531–545.

Sharqawy, M., Lienhard, J., Zubair, S.M., 2010. Thermophysical properties of seawater: a review of existing correlations and data, desalination and water treatment. Desalin. Water Treat. 16, 354–380.

Toll, N., Rasmussen, T., 2007. Removal of barometric pressure effects and Earth tides from observed water levels. Ground Water 45 (1), 101–105.

Turcotte, D.L., Schubert, G., 2014. Geodynamics. University Press, Cambridge.

Valley, B., 2007. The Relation Between Natural Fracturing and Stress Heterogeneities in Deep-seated Crystalline Rocks at Soultz-sous-Forêts (France). ETH Zurich (Ph D. Thesis).

Vidal, J., Genter, A., Schmittbuhl, J., 2015. How permeable fractures in the Triassic sediments of Northern Alsace chracaterize the top of hydrothermal convective cells? Evidences from Soultz geothermal boreholes (France). Geotherm. Energy J. 3 (8), http://dx.doi.org/10.1186/s40517-015-0026-4, Special Issue: Characterization of Deep Geothermal Systems.

Vidal, J., Genter, A., Schmittbuhl, J., 2016. Pre- and post-stimulation characterization of geothermal well GRT-1, Rittershoffen, France: insights from acoustic image logs of hard fractured rock. Geophys. J. Int. 206 (2), 845–860, http://dx.doi.org/10.1093/gji/ggw181.